JOURNAL OF
EMERGING INVESTIGATORS

Article

Analysis of the effects of positive ions and boundary layer temperature at various hypersonic speeds on boundary layer density

Akash Selvakumar[1], Sridhar Palanisamy[2]
[1]North Creek High School, Bothell, Washington, USA
[2]Karpagam University, Coimbatore, India

SUMMARY

Vehicles traveling at hypersonic speeds ionize the air around them. This ionization leads to the possibility of utilizing an induced positive surface charge to lower the density of the boundary layer flow electrostatically. Reducing the boundary layer's density would have several positive effects, such as lowering the drag and heat transfer. The study's goal was to identify the Mach numbers for which the electrostatic drag and heat transfer manipulation would be most applicable inside the stratosphere. We hypothesized that the potential to use induced positive surface charge repulsion to lower boundary layer density would increase with speed, and there will be greater (>10%) potential to decrease boundary layer density at a lower bound estimate of Mach 18-19. We also explored the extent to which extrapolation through a quadratic model based on Dr. Jesse R. Maxwell's data in *Morphing Waveriders for Atmospheric Entry* could be used to approximate maximum boundary layer temperature values. The experiments were conducted using computational fluid dynamics software. The study demonstrated that, on average, higher Mach speeds resulted in a considerably higher potential decrease in density. Also, as predicted by the hypothesis, a significant potential reduction in density occurred near Mach 19. The study also supported using the quadratic model based on Maxwell's data for approximating the maximum boundary layer temperature up to at least Mach 26. This study highlights that further research on the surface charge method is warranted as we seek to explore higher hypersonic speeds within the stratosphere.

INTRODUCTION

The desire to achieve higher speeds is a constant fascination with humans. As we delve into the hypersonic spectrum, there is a constant search for ways to further increase the speed of our atmospheric vehicles. In order to do so, it is essential we identify methods to reduce drag and lower the convective heat transfer(heat transfer from the surrounding hot air to the vehicle), which can be fatal to vehicle bodies located inside the extreme temperatures present in hypersonic airflows. One way to achieve a reduction in skin drag and convective heat transfer is through decreasing the density of the boundary layer. Decreasing the density of the boundary layer leads to a reduction in skin friction and thus a reduction in skin drag (1). Convective heat transfer can be considered as the combined effects of conduction and fluid motion (advective) heat transfer (2). The heat flux φ_q for advective heat transfer is modelled by the equation:

$$\varphi_q = v\rho c_p \Delta T$$

where ρ is density, c_p is heat capacity at constant pressure, ΔT is the difference in temperature, and v is velocity. Thus, changing the density of flow inside the boundary layer (near the surface of the vehicle) the advective and thus convective heat transfer is decreased.

Our study considered the induced surface charge repulsion method for lowering boundary layer density (3). Inducing positive surface charge on the vehicle will electrostatically repel positive ions and thus lower boundary layer density (3). The maximum potential reduction in boundary layer density through induced surface charge, which will be calculated for specified trails in the experiment, will thus be equivalent to the percentage of the density that can be attributed to positive ions.

We performed a study to analyze the maximum potential reduction in the boundary layer possible by positive surface charge repulsion at various speeds. The study utilized the Ansys Fluent Computational Fluid Dynamic Software to perform several trials at different Mach numbers (a dimensionless measurement of speed with respect to the local speed of sound) and gather average boundary layer static temperature data. We repeated each trial twice and averaged the results to produce reliable data. This data was then analyzed to answer questions regarding the relationship between Mach number and maximum potential density decrease by induced positive surface charge repulsion. Furthermore, we analyzed the data to validate a proposed model and understand the relationship between boundary layer temperature and Mach number. The method of induced

charge has a primary application in the high hypersonic spectrum because the air is not at high enough temperatures to be ionized at subsonic, supersonic, and low hypersonic speed ranges in regular air conditions, rendering the effect of electrostatically repulsion negligible (4-5).

Temperature is a measurement of the average kinetic energy(6). When a vehicle moves through air it transfers some of its kinetic energy to the particles around it via collisions (7). The amount of kinetic energy gained by the particles is proportional to the kinetic energy of the vehicle. Therefore, air particles around vehicles traveling at higher velocities gain more kinetic energy and temperature (7). Since increasing temperature of the air results in increased ionization of the air particles (4), we hypothesized that the potential for the induced positive surface charge method to lower boundary layer density will increase with speed. Upon performing our CFD study, we demonstrated that, on average, higher Mach speeds resulted in a considerably higher potential decrease in density supporting this hypothesis.

RESULTS

Preliminary Estimate

A study done by Maxwell provided the maximum temperature values inside the boundary layer for vehicles traveling inside the stratosphere at speeds up to Mach 10 (5). To estimate maximum boundary layer temperature values at Mach numbers greater than 10, we performed quadratic regression. From the quadratic regression, we determined the quadratic best fit function for Maxwell's data to be:

$$T(s) = 196 + 43.9s + 23.8s^2$$

where ***T*** is the maximum boundary layer temperature and ***s*** is the Mach number (**Figure 1**).

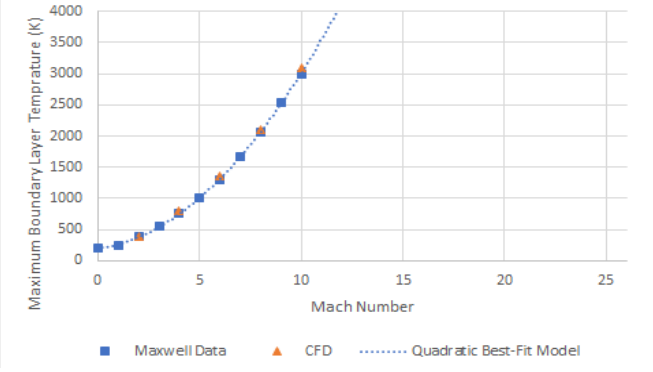

Figure 1. Comparison of published experimental and CFD maximum boundary temperature values. The Quadratic Best fit model (dotted blue line) based on Maxwell's published maximum boundary layer data (5) is included to show extrapolation to higher values. The Graph illustrates the closeness between the Quadratic model estimates, Maxwell's maximum boundary layer temperature values (blue squares), and CFD maximum boundary temperature values (orange triangles).

Table 1. Comparison of CFD estimates, published experimental data, and quadratic model predictions of maximum boundary layer temperature at lower Mach numbers.

Mach Number	CFD Maximum Boundary Layer Temperature Values (K)	Maxwell Maximum Boundary Layer Temperature Values (K)	Quadratic Best Fit Model Maximum Boundary Layer Temperature Estimates (K)	Percent Deviation of CFD Maximum Boundary Layer Temperature Values from Maxwell Values (%)	Percent Deviation of Quadratic Model Maximum Boundary Layer Temperature Estimates from Maxwell Values (%)
2	390.16	380	379.0	2.67	0.26
4	794.34	770	752.4	3.16	2.29
6	1359.79	1300	1316.2	4.60	1.25
8	2096.45	2070	2070.4	1.28	0.02
10	3097.96	3000	3015.0	3.27	0.50

This quadratic model closely adheres to Maxwell's data (**Table 1**). From previous Computational Fluid Dynamics (CFD) static temperature simulation results, we observed that a significant portion of the boundary layer is near the maximum boundary layer temperature (5). By using this quadratic model for the maximum temperature inside the boundary layer (**Figure 1**), we can also hypothesize that a lower-bound approximate value of Mach 18-19 from which we will see a significant (For our study we are defining 10% and above as significant since our educated assumption is that this level of reduction will produce measurable effects in drag and convective heat transfer reduction) decrease in drag and convective heat transfer.

As predicted by this hypothesis, we ascertained that a significant (10% or greater) potential reduction in density occurred near Mach 19. Furthermore, the study provided reasonable support for using the above quadratic best fit function for estimating maximum boundary layer temperature.

CFD Study

The potential reduction in boundary layer density through positive surface charge and its variance in regard to vehicle speed was determined by first identifying the average temperature of the boundary layer at various Mach speeds. The average boundary layer temperature was identified through utilizing the Ansys Fluent CFD software to simulate the vehicle moving at various speeds at an altitude of 25 km above sea level and for each Mach number simulation we selected 20 points for temperature reading evenly spaced throughout the boundary layer to get a good measurement for the average temperature within the boundary layer (**Figure 2**). The average temperature data was further used to determine the percent decrease in density potentially achievable by induced surface charge repulsion for each trial.

Furthermore, the quadratic model for maximum boundary layer temperature was validated by using the CFD simulation to identify the point of maximum boundary layer temperature. This point was identified by taking the temperature at the surface of the vehicle towards the tip of the cone. Preliminary CFD trials were performed at Mach 2, 4, 6, 8, and 10. The CFD maximum boundary layer temperature data showed strong adherence with previous experimentation published in Maxwell's study (**Table 1**), which strengthened the validity of

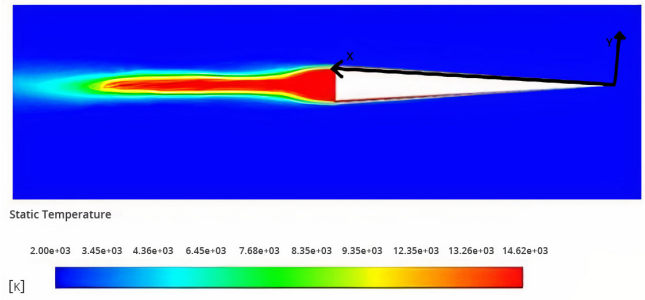

Figure 2. CFD Static Temperature Data for Mach 24. The x and y axis on the CFD temperature diagram show the position axis used to determine points for data collection. The diagram also shows the static temperature values (K) for the air around the vehicle.

this study. Afterwards, trials were performed for Mach 12, 14, 16, 18, 20, 22, 24, and 26. Additional trials were conducted at Mach 19, 21, 23 to understand the data better and identify a more exact Mach number for significant air drag reduction. The potential boundary layer density decrease was not calculated for Mach 14 and lower because the ionization of air is negligible for average temperature values lower than 6000 K (7).

On average, increasing Mach number resulted in a significant increase in average boundary layer temperature and a considerable potential decrease in boundary layer density (**Table 2**). The data also indicates that the lowest Mach number with a significant (10% or greater) potential reduction in boundary layer density occurs at slightly less than Mach 19. Thus, based on the CFD data, the lowest whole Mach number with a significant potential decrease in density will be Mach 19.

To validate the quadratic model, a mean percent error (MPE) of 3.209% was seen for the extrapolation model values compared to the actual data for maximum boundary layer temperature gathered by the CFD (**Table 3**). Furthermore, the average percentage deviation of the Maximum Boundary layer Temperature from Average Boundary Layer Temperature (**Table 3)** was 7.363%.

DISCUSSION

The study was performed to understand the relationship between Mach number and boundary layer temperature and ion density. This was used to determine the potential applicability of induced positive surface charge repulsion to lower boundary layer density. The results of this study's experimentation were supported by the strong adherence of the study's CFD determined maximum boundary layer temperature values to previously determined maximum boundary layer temperature values (5) (**Table 1**). The trials conducted supported the hypothesis that the potential to use induced positive surface charge repulsion to lower boundary layer density would increase with speed, and there will be significant (>10% density decrease) potential to decrease boundary layer density at a lower bound estimate of Mach 18-19. From the results, we can observe that increasing the Mach number results in a greater potential to decrease boundary layer density using induced surface charge. The data also showed that a greater than 10 percent potential decrease in density occurring at Mach 19. Thus, we can ascertain that at speeds greater than or equal to Mach 19, inside the stratosphere, there will be significant potential to decrease boundary layer density through repelling the positive ions in the boundary layer. Speeds of upwards Mach 9 have already been reached inside the stratosphere (8), while speeds of up to Mach 17 - 22 have been reached by aircraft at higher altitudes (9). Predictions for scramjet-powered aircraft, which operate inside the stratosphere, indicate that speeds of Mach 20 and above are achievable (10). Therefore, while this positive surface charge method is not currently applicable for stratosphere flight, this may change in the future. For instance, the induced surface charge method may have application in future military hypersonic vehicles and weapon systems traveling at very high hypersonic speeds that seek to operate at shallower trajectories inside the lower atmosphere (stratosphere) to avoid interception.

The quadratic model's predictions for maximum boundary layer temperature values at higher Mach numbers seem to be closely correlated with CFD reading. This indicates

Table 2. Data and results for determination of maximum potential percentage reduction in boundary layer density by positive surface charge at various Mach numbers.

Mach Number	Average Boundary Layer Temperature (K)	Percent Potential Decrease in Density (%)
16	6501.89	0.19
18	8469.74	4.22
19	9348.07	12.05
20	10347.45	33.03
21	11257.44	56.76
22	11715.59	64.15
23	13259.22	91.83
24	13818.99	95.71
26	17958.88	99.85

Table 3. Data for validation of quadratic model for maximum boundary layer temperature and analysis of Boundary Layer temperature

Mach Number	CFD Average Boundary Layer Temperature (K)	CFD Maximum Boundary Layer Temperature (K)	Quadratic Model Values for Maximum Boundary Layer Temperature (K)	Percent Error for Quadratic Model Results and CFD Maximum Boundary layer Temperature (%)	Percent Deviation of Maximum Boundary Layer Temperature from Average Boundary Layer Temperature (%)
2	354.16	390.16	379.00	2.86036	10.16505
4	734.36	794.34	752.40	5.27985	8.16766
6	1269.66	1359.79	1316.20	3.20564	7.09913
8	1942.86	2096.45	2070.40	1.24258	7.90549
10	2943.34	3097.96	3015.00	2.67789	5.25309
12	4118.32	4341.95	4150.00	4.42082	5.43005
14	5229.6185	5766.92	5475.40	5.05504	10.2742
16	6501.8925	7066.22	6991.20	1.06167	8.67943
18	8469.74	8998.36	8697.40	3.34461	6.24123
19	9348.07	9898.16	9621.90	2.79102	5.88451
20	10347.45	10921.80	10594.00	3.00134	5.55068
21	11257.44	11956.32	11613.70	2.86560	6.20813
22	11715.59	13180.35	12681.00	3.78859	12.50266
23	13259.22	13956.33	13795.90	1.14951	5.25755
24	13818.99	14876.24	14958.40	0.55229	7.65070
26	17958.88	18952.57	17426.20	8.05363	5.53314

that this quadratic model may be a reasonable method for approximating the maximum boundary temperature up to at least Mach 26. Additionally, the percent deviation of the maximum boundary layer temperature from the average boundary layer temperature seems to validate the observation that a significant portion of the boundary layer is near maximum boundary layer temperature. On average, a low standard deviation of less than 10 percent was observed. This observation highlights the possibility that maximum boundary layer temperature can be used as a rough estimate for the average boundary layer temperature at high Mach numbers. However, further study and additional trials would be necessary to validate this claim thoroughly.

A primary cause for fluctuations in the data can be attributed to the number of iterations that were run for each simulation. The higher the iterations the more accurate the CFD data; though $5x10^5$ iterations were performed, there may still be some inaccuracies thus resulting in fluctuations in the data. There could also be a slight variation in the placement of the cursor when recording data points. This variation would primarily serve to affect the maximum boundary layer temperature readings from the CFD, where the cursor must be located at the tip of the cone near the surface (leading edge) (11), by giving data points lower than the actual maximum. Finally, some errors in determining the maximum potential density decrease may result from using the concentration graph. The graph provides reasonably accurate estimates based on previous studies, and the manual identification process may result in some error.

It is important to note that the study used the average boundary layer temperature to get the percent density of the mixture that can be attributed to positive ions. This method would only serve to give an approximate answer. A more accurate means of identifying the density percentage is by calculating the percent density attributed to positive ions at each point and integrating through the entirety of the boundary layer. Since this operation would be impractical with the method of density identification used for this project, it was not used. However, if coupled with another percent density identification method, such as the Saha ionization equation method, this method could determine even more accurate data for future research. Furthermore, in future studies using CFDs, more accurate density change approximation may be achieved with the Saha ionization equation. This equation becomes applicable for relatively low ionization plasmas, as is the case with the air inside the boundary layer. When solved as a system of equations alongside a simple density relationship, the Saha ionization equation could better estimate the maximum density change possible at a given temperature and boundary layer density.

Further research with wind tunnels and the physically inducing charge would substantially contribute to this experiment. Physical experiments would allow us to examine a wide variety of data and thus would help get quantitative answers to questions regarding the effect of positive surface charge on air drag and convective heat transfer. Physical experiments will also be the best approach to identify the amount of positive surface charge needed to achieve significant effects and allow for research into various charge distributions to optimize effects. For example, further physical research can be performed to optimize charge distributions to optimize the decrease in heat transfer while lowering the decrease in drag for application of induced charge during reentry of spacecraft. Additional research with CFDs could consider the potential effect of positive surface charge in reducing the air density in front of the vehicle. Using a positive surface charge to reduce the perceived freestream density of the flow would have significant and already quantified effects on drag and convective heat transfer (12). However, since the temperature in front of the vehicle is considerably lower than the temperatures inside the boundary layer, much higher speeds would be necessary to produce the same density reduction. However, this research could have applications for future extremely fast hypersonic vehicles.

METHODS

Computational Fluid Dynamic Analysis

Solidworks was used to create a mesh of the hypersonic vehicle for the simulation. The vehicle was modeled by a cone, which is an effective model for hypersonic vehicle bodies (13). The cone was created to the specified dimensions of 5 m length and 0.5 m radius. The objects properties were defined as solid. The Ansys Fluent CFD environment was used to model the temperature of the air inside the boundary layer. The Solidworks mesh of the hypersonic vehicle was imported into the CFD. We configured the CFD simulation as Hypersonic flow at an altitude (25 km above sea level) and set the specified Mach number for the trial. Each trial was set to have 5x10^5 iterations performed to get accurate results. The simulation was set to return the velocity and static temperature data. Each trial was repeated twice with collected data averaged to reduce error.

Trials were held at Mach Numbers 2, 4, 6, 8, 10, 12, 14, 16, 18, 19, 20, 21, 22, 23, 24, 26. The trials at 2, 4, 6, 8, 10 served as preliminary trials to verify the accuracy of our CFD simulations. The velocity data was used to approximate the width of the boundary layer (**Figure 3**). The boundary layer is the area in which the velocity of the flow is changed by

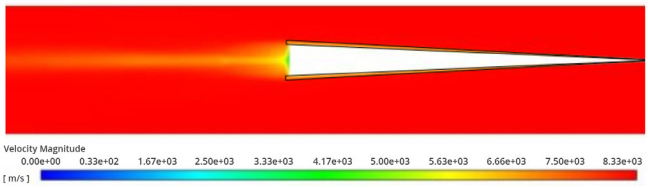

Figure 3. CFD Velocity Data for Mach 24. The boundary layer is outlined in black on a CFD velocity diagram. The diagram shows the velocity of the air (m/s) around the vehicle relative to the vehicle.

the viscous interactions (14). Thus, the areas in the data around the sides of the vehicle where the velocity changed thus indicated the boundary layer. An outline of the boundary layer was made and overlaid on the static temperature data reading indicating the whereabouts of the boundary layer for accurate data collection.

Average Boundary Temperature Identification

With the boundary layer marked, 20 points were chosen by hand evenly within the boundary. Due to symmetry, the points were taken at the upper boundary layer (**Figure 3**). We set the position axis with the x axis as distance in meters from the origin located at the tip of the vehicle and the y axis as distance in meters from the vehicle (**Figure 2**). The points were chosen at roughly 0.0, 0.5, 1.0, 1.5, 2.0, 2.5, 3.0, 3.5, 4.0, 4.5, 5.0, 5.5 as x values and y values varying evenly within the boundary layer. The number of points chosen at each value vary proportionately with the thickness of the boundary layer at each x value. Taking an average of the static temperature values at these points was used to produce a good estimate for the average temperature within the boundary layer.

Maximum Boundary Layer Temperature Identification and Calculations

The maximum boundary layer temperature was identified by taking the value at the point (0,0) utilizing the position axis defined above (**Figure 2**). This gives the value at the leading edge and tip of the cone where the temperature is the highest (11). Percent error calculation of quadratic model data for CFD maximum boundary layer temperature was calculated by the equation:

$$\%e = |T_m - T_c|/T_c \times 100\%$$

where T_m is the maximum boundary layer temperature calculated from the quadratic model and T_c is the maximum boundary layer temperature obtained from the CFD simulation. The percent deviation of maximum boundary layer temperature from average boundary layer temperature was calculated similarly using the equation:

$$\delta = |T_z - T_c|/T_a \times 100\%$$

where T_a is the average boundary layer temperature obtained from the CFD simulation and T_c is the maximum boundary layer temperature obtained from the CFD simulation. Similar calculations were performed for the percent deviation of CFD simulation maximum boundary layer temperature values and Quadratic Model maximum boundary layer temperature estimates from Maxwell's maximum boundary layer temperature values.

Maximum Potential Percent Decrease in Boundary Layer Density Calculation

The concentration of positive ions inside the boundary layer was determined based on a temperature concentration graph provided by Professor J. E. Shepherd for air, based on experimental data (**Table 2**) (4). This graph was utilized to get a rough estimate for the percentage of the density attributed to positive ionic species. The maximum potential percent decrease in density by positive surface charge repulsion is equivalent to the percentage of the density attributed to positive ions. Thus, the maximum potential percent decrease in density by positive surface charge repulsion is ($\%\Delta\rho$) was thus identified by the equation:

$$\%\Delta\rho = (\Sigma m_n C_i)/(\Sigma m_n C_n + \Sigma m_i C_i)$$

where $\Sigma m_i C_i$ is the summation across all positive ions of the molar mass of each positive ion multiplied by the number concentration of each ion, $\Sigma m_n C_n$ is the summation across all species that are not positive ions of the molar mass of the species multiplied by the number density of the species.

ACKNOWLEDGMENTS

I would like to thank my parents for supporting me through the research, paper writing, and submission process. I am very grateful for Professor J. E. Shepherd for taking the time to provide me with the necessary information to calculate ion concentration. I would also like to thank Mr. Henning for helping me through some of the complex math when I was gaining preliminary understanding of the topic. Finally, I would like to thank Ms. Haupt for teaching the data analysis and scientific paper writing skills that were extremely helpful for this research.

Received: July 11, 2020
Accepted: September 24, 2020
Published: October 2, 2020

REFERENCES

1. Suraweera, M. V., Mee, D. J., & Stalker, R. J. "Skin Friction Reduction in Hypersonic Turbulent Flow by Boundary Layer Combustion." American Institute of Aeronautics and Astronautics, 2005, pp. 9-10.
2. "Convection Heat Transfer." *McGraw-Hill Higher Education*, McGrawHill Education, www.mhhe.com/engcs/mech/cengel/notes/ConvectionHeatTransfer.html.
3. Tajmar, Martin. *Advanced Space Propulsion Systems.* Springer-Verlag, 2003.
4. Shepherd, J. E. "Re: Request for information/guidance - Sub: Saha ionization" Received by Akash Selvakumar, Jun 18, 2020. E-mail Communication.
5. Maxwell, Jesse R. *Morphing Waveriders for Atmospheric entry*. 2019. University of Maryland, PhD dissertation.

DRUM, https://drum.lib.umd.edu/handle/1903/21909.
6. "Temperature and Kinetic Energy." Chemistry 301, University of Texas, ch301.cm.utexas.edu/section2.php?target=gases%2Fkmt%2Ftemp-kinetic-energy.html.
7. Atluri, S. N., *et al*. *Computational Mechanics '95 Volume 1 and Volume 2 Theory and Applications*. Springer Berlin, 2014.
8. Martin, Guy. "Hypersonic Pioneer: The X-43A." Aircraft Information, www.aircraftinformation.info/art_x43.htm.
9. Acton, James M. "Hypersonic Boost-Glide Weapons." Routledge Taylor & Francis Group, 2015, pp. 203–204, scienceandglobalsecurity.org/archive/2015/09/hypersonic_boost-glide_weapons.html.
10. McClinton, Charles. "X-43: Scramjet Power Breaks the Hypersonic Barrier." Dryden Lecture. 44th AIAA Aerospace Sciences Meeting and Exhibit, 9 Jan. 2006, Reno, Nevada, web.archive.org/web/20110724231440/http://www.aiaa.org/Participate/Uploads/AIAA_DL_McClinton.pdf.
11. Kasen, Scott D. *Thermal Management at Hypersonic Leading Edges*. 2013. University of Virginia, PhD dissertation
12. Hanquist, Kyle M., and Iain D. Boyd. "Plasma Assisted Cooling of Hot Surfaces on Hypersonic Vehicles." Frontiers in Physics, Plasma Physics, Frontiers, 17 Jan. 2019, www.frontiersin.org/articles/10.3389/fphy.2019.00009/full.
13. Ahmed, Waqas *et al*. "Hypersonic Flow over Cone and Wedge in context of Hypersonic Vehicle Design using CFD". IBCAST 34. 2010.
14. Epifanov, V. M. "BOUNDARY LAYER." THERMOPEDIA, thermopedia.com/content/595/.